Organoborane Macrocycles

Deutsche Ausgabe: DOI: 10.1002/ange.201503219
Internationale Ausgabe: DOI: 10.1002/anie.201503219

Versatile Design Principles for Facile Access to Unstrained Conjugated Organoborane Macrocycles**

*Pangkuan Chen, Xiaodong Yin, Nurcan Baser-Kirazli, and Frieder Jäkle**

Abstract: *A facile and versatile approach was developed to access ambipolar boron-containing macrocycles. Two examples of new conjugated cyclic motifs are presented with carbazole moieties as donors and borane moieties as acceptors embedded into the ring system. They were first predicted using computational methods. Possible targets with appropriately shaped π-conjugated bridges that minimize the overall ring strain were identified and their geometry was optimized by DFT methods. The synthetic demonstration was then accomplished using organometallic condensation reactions under high dilution conditions. The resulting monodisperse macrocycles provide important insights into the design principles necessary for the preparation of new unstrained macrocycles with interesting optical and electronic characteristics. The current research also offers a more general approach to conjugated ambipolar B/N macrocycles as a promising new family of (opto)electronic materials.*

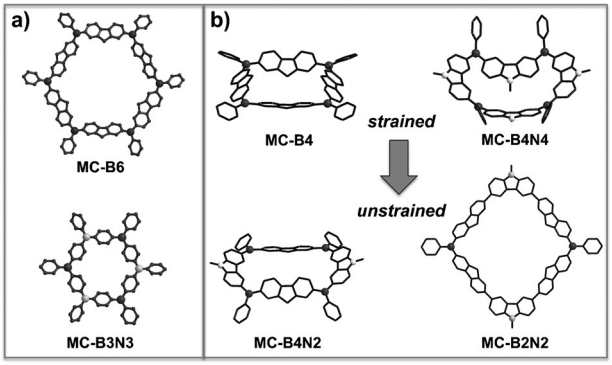

Scheme 1. DFT-optimized structures (B3LYP/6-31G*) of boron-containing conjugated macrocycles (B = dark gray, N = light gray spheres). a) Previously reported unstrained macrocycles **MC-B6** and **MC-B3N3**; b) **MC-B4N2** and **MC-B2N2** obtained in this work by structural modification of strained macrocycles **MC-B4** and **MC-B4N4**.

Conjugated materials continue to attract immense research interest, motivated by potential applications in molecular electronics, energy, chemical sensors, and biomedical fields.[1] A recent focus on conjugated macrocycles has been triggered by the expectation that favorable (and different) properties and functions can be achieved owing to their unique structural features.[2] Thus, the synthesis, electronic features, supramolecular assembly, and host–guest interactions of shape-persistent conjugated macrocycles have been investigated extensively.[3] An attractive current direction is the incorporation of heteroatoms into π-conjugated carbon-based cycles that provide added functionality and may enable new applications.[4] In 2010, Ito, Tanaka, and co-workers reported an interesting example of a hexaaza[1_6]paracyclophane, an electron-rich macrocycle with an unusual electronic structure and intriguing redox properties.[5,6] Our group recently developed a "charge-reverse"[7] electron-deficient hexaboracyclophane, **MC-B6**,[8] and an ambipolar macrocycle, **MC-B3N3**,[9] in which electron-rich arylamines alternate with electron-deficient arylboranes (Scheme 1 a). These macrocycles are unique representatives of the larger class of conjugated organoboranes, which have attracted tremendous interest in recent years for applications in non-linear optics, organic light emitting devices, as photochromic smart materials, in the detection of anions, and many other fields.[10]

The synthetic access to fully conjugated macrocycles can pose significant challenges, which is especially true when the intrinsic ring strain energy of the products disfavors the cyclization process.[11] Realizing that the trigonal coordination geometry in organoboranes should favor sixfold symmetry, we previously targeted hexameric macrocycles with B or N at the six corners and linear aromatic moieties as π-conjugated linkers.[8,9,12] The macrocycle **MC-B6** was obtained in high yield, but the cyclic tetramer **MC-B4** as a smaller analogue could not be generated selectively and, although detected by MALDI-MS, its isolation proved to be problematic.[8] To systematically uncover the reasons for these findings, DFT (B3LYP/6-31G*) computational studies were performed on all the macrocycles (Scheme 1). Analysis of the geometric parameters revealed that ring strain is reflected in deviations of the endocyclic C-B-C angles (θ) from 120.0° and distortions of the individual π-building blocks as measured by the interplanar angle (δ) between the six-membered rings of fluorene (0° for unstrained compounds). The calculated C-B-C angles of 120.3° in **MC-B6** and 119.8° in **MC-B3N3** are close to the ideal value of 120.0°, and the fluorenes in the former show little evidence of distortions ($\delta = 0.6°$). In contrast, a smaller angle of $\theta = 118.1°$ at boron was predicted for **MC-B4** and large distortions of the fluorene moieties ($\delta = 6.1°$) are indicative of pronounced ring strain.

Therefore, we decided to explore methods to modify the unfavorable structure of tetrameric **MC-B4** to reduce the strain energy in this smaller cyclic system. 2,7-Disubstituted

[*] Dr. P. Chen, Dr. X. Yin, N. Baser-Kirazli, Prof. Dr. F. Jäkle
Department of Chemistry, Rutgers University, Newark
73 Warren Street, Newark, NJ 07102 (USA)
E-mail: fjaekle@rutgers.edu
Homepage: http://chemistry.rutgers.edu/fjaekle/

[**] This material is based upon work supported by the National Science Foundation under Grants CHE-1112195 and CHE-1362460.

Supporting information for this article is available on the WWW under http://dx.doi.org/10.1002/anie.201503219.

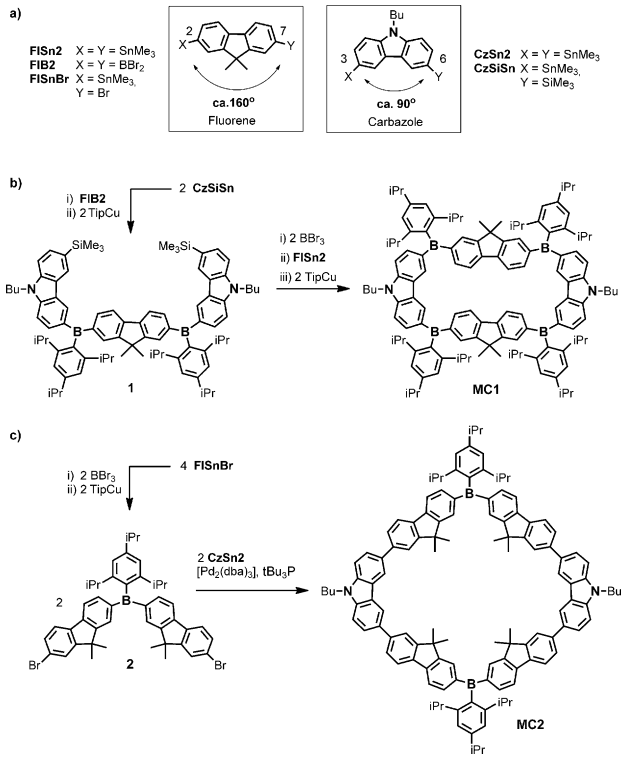

Scheme 2. Structures of π-building blocks used in this work and synthesis of macrocycles **MC1** and **MC2**.

fluorene and 3,6-disubstituted carbazole offer very different geometries with a preferred angle close to 160° for the former and a much smaller angle of ca. 90° for the latter (Scheme 2a). Two possible approaches were considered to achieve less-strained macrocycles: First, the carbazole moiety as a bent π-conjugated linker can be used to replace some of the more linear fluorene moieties, without changing the position of the boron atoms. Another approach is to replace some of the boranes themselves (120°) with carbazole moieties (90°) while retaining the fluorene bridges in the macrocycle. To test our hypothesis, we again performed DFT calculations. The results indicated that replacement of all the fluorene π-bridges with carbazoles leads to a macrocycle **MC-B4N4** that is also highly strained ($\theta = 119.0°$, $\delta = 5.3, 8.1°$) because the angles become too small (Scheme 1b). However, if only two of the fluorenes are replaced, a hybrid macrocycle (**MC-B4N2**) is generated, which shows a value of $\theta = 120.9°$ and almost undistorted fluorene ($\delta = 2.0°$) and carbazole ($\delta = 1.0°$) bridges. Similarly, replacement of two borane moieties in **MC-B4** with carbazoles results in a macrocycle (**MC-B2N2**) with little strain that should be easily accessible given the predicted values of $\theta = 120.3°$ and $\delta = 2.0°$ (fluorene), 0.8° (carbazole).

Synthetic access to **MC1** involves preparation of the silylated oligomer **1**, which was then reacted with two equivalents of BBr_3 (Scheme 2b). Macrocyclization was accomplished by an organometallic condensation between the resulting borylated species and the stannyl groups of 2,7-bis(trimethylstannyl)-9,9-dimethylfluorene (**FlSn2**) under pseudo high-dilution conditions. The initially generated boron halide functionalized macrocycle was then treated with two equivalents of the organocopper reagent TipCu (Tip = 2,4,6-triisopropylphenyl) in refluxing toluene to introduce the Tip moieties as bulky groups for steric protection of boron. Analysis by gel permeation chromatography (GPC) indicated that the crude sample after standard workup consists of the targeted macrocycle as the major product. A higher molecular weight component was also observed, which likely corresponds to a larger cyclic (or linear) species (Supporting Information, Figure S1). Further purification by preparative size-exclusion column chromatography on Biobeads with THF as the eluent gave analytically pure **MC1** as a white powdery material.

For the synthesis of **MC2**, the brominated borane species bis(2-bromo-9,9-dimethylfluoren-7-yl)(triisopropylphenyl)-borane (**2**) was first prepared. Macrocyclization was achieved by Pd-catalyzed Stille coupling of **2** and 3,6-bis(trimethylstannyl)carbazole (**CzSn2**) under highly dilute conditions. The resulting macrocycle **MC2** was purified using a similar procedure as described for **MC1**. Thanks to the steric shielding effect of the bulky Tip groups, the products show good stability to air and moisture in the solid state and can be handled in non-polar solvent for several days without significant decomposition.

GPC measurements on the purified products **MC1** and **MC2** revealed narrow bands indicating monodisperse products (Supporting Information, Figures S1, S2). Formation of the desired macrocycles was further confirmed by high-resolution MALDI-MS spectroscopy, which showed the expected molecular ion peaks at $m/z = 1683.1936$ for **MC1** and at $m/z = 1638.9879$ for **MC2**. These numbers are very close to the theoretically predicted values (Supporting Information, Figure S3). As expected, given the symmetry of the macrocycles, the ^{1}H NMR spectrum for **MC1** shows only two singlets and four doublets in the aromatic region that are assigned to the fluorene and carbazole groups (Figure 1a; Supporting Information, Figure S4). The number of signals

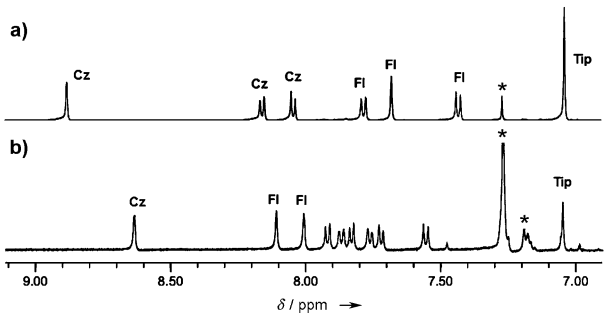

Figure 1. Aromatic region of the ^{1}H NMR spectra of a) **MC1** and b) **MC2** (* denotes $CHCl_3$ and residual toluene).

for **MC2** is also consistent with the predicted structure; an additional singlet and two doublets compared to **MC1** are due to the chemical nonequivalence of the protons in the fluorene moiety (Figure 1b; Supporting Information, Figure S7).

The optical properties were examined in solvents of different polarity to gain insights into the photophysical and charge transfer characteristics. The UV/Vis absorptions in

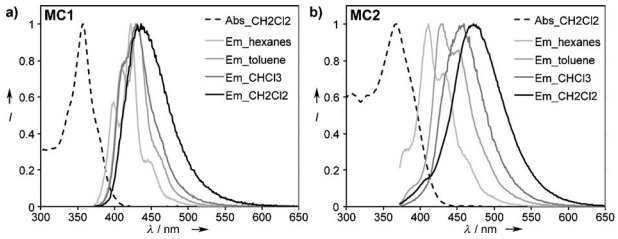

Figure 2. UV/Vis absorption (Abs) and emission (Em) spectra for **MC1** and **MC2** (excited at $\lambda_{abs,max}$).

CH_2Cl_2 with maxima at 357 nm for **MC1** and 367 nm for **MC2** are ascribed to intramolecular charge transfer (ICT) from the carbazole donor (n/π) to fluoreneborane acceptor sites (n/π*) (Figure 2). The absorption data of **MC1** and **MC2** proved to be essentially independent of the solvent polarity. In contrast, the emission bands of **MC1** (CH_2Cl_2: $\lambda_{fl} = 436$ nm, $\Phi_{fl} = 0.40$, $\tau_{fl} = 6.22$ ns) and **MC2** (CH_2Cl_2: $\lambda_{em} = 474$ nm, $\Phi_{fl} = 0.37$, $\tau_{fl} = 2.74$ ns) experienced a strong bathochromic shift as the solvent polarity was increased (Supporting Information, Figure S10, S11). Vibronic fine-structure was observed only in low-polarity solvents. The solvatochromic effect in the emission, but only small effect in the absorption, is attributed to an increase in polarity of the excited state upon ICT. This phenomenon is typical of Ar_2B-π-NAr_2 systems and similar to what we previously observed for **MC-B3N3**.[9] The onsets of absorption at 390 nm in **MC1** and 427 nm in **MC2** are well reproduced by the vertical excitation data of 382 and 409 nm determined by TDDFT calculations (see below).

Computational studies (DFT; B3LYP/6-31G*)[13] were carried out on simplified analogs of **MC1** in C_{2V} and **MC2** in C_2 symmetry (Me and *i*Pr groups are replaced with H, and *n*Bu groups on carbazole with Me groups) and the results are summarized in the Supporting Information, Table S1, S2. As mentioned before, the endocyclic bond angles about boron for **MC1** (120.9°) and **MC2** (120.3°) are calculated to be much closer to 120° than that for **MC-B4** (118.1°), leading to formation of less strained cyclic motifs. In **MC1**, the HOMO (−5.41 eV) is localized mostly on the carbazole moieties, while the LUMO (−1.87 eV) shows delocalization over the conjugated π-systems of the fluorene units and the boron centers with only small contributions from the carbazole moieties (Figure 3). Similar contributions from carbazole and fluorene donors are identified for the HOMO (−5.06 eV) in **MC2**, but the LUMO (−1.77 eV) is predominantly centered on the two boron sites. A relatively higher HOMO level in **MC2** is attributed to the direct attachment of the electron-donating fluorene units to the carbazole moieties. As typically observed for symmetric macrocycles, the $S_1 \leftarrow S_0$ transition is symmetry-forbidden because of cancellation of the transition dipole moments in the ring structures.[14] Instead, higher energy transitions, including S_2, S_3, $S_4 \leftarrow S_0$ for **MC1** and S_2, S_3, $S_5 \leftarrow S_0$ for **MC2**, are believed to correspond to the experimentally observed absorptions. Besides the HOMO and LUMO, other orbitals that play a role in these transitions include the HOMO−1, HOMO−2, and LUMO+1 (Supporting Information, Figure S14, S15). The fact that these macrocycles are strongly emissive is indicative of structural relaxation and possibly exciton localization in the ICT excited state.[14c]

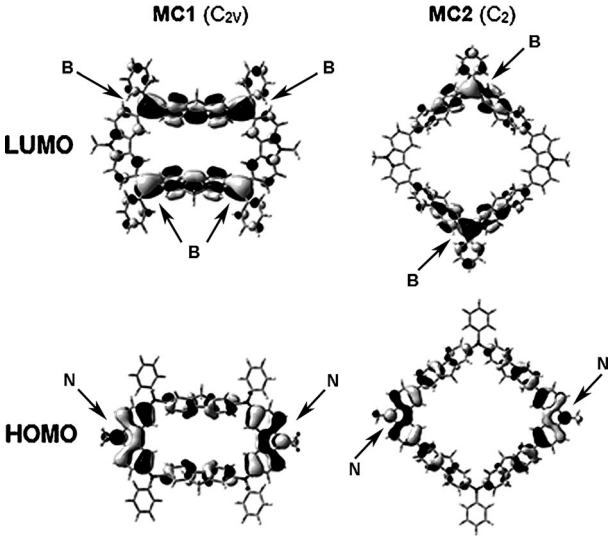

Figure 3. Computed HOMO and LUMO orbital plots for **MC1** (C_{2V}) and **MC2** (C_2) in the ground state (B3LYP, 6-31G*, isovalue = 0.2). Me groups on fluorene and *i*Pr on Tip are replaced with H. *n*Bu groups on carbazole are replaced with Me.

The frontier orbital energy levels of **MC1** and **MC2** were also probed by cyclic and square-wave voltammetry (Figure 4; Supporting Information, Figure S18). For **MC1**, a single irreversible oxidation wave at 0.95 V was recorded in CH_2Cl_2, which suggests very weak or no electronic communication between the nitrogen atoms on opposite sides of the cycle. A similar oxidation process is also observed for **MC2**, but at a lower potential of 0.61 V. The reason for the difference in redox potential might be that the direct attachment of the borane acceptors in **MC1** lowers the electron density on the carbazole moieties. Four separate, reversible reduction waves are observed for the borane moieties in

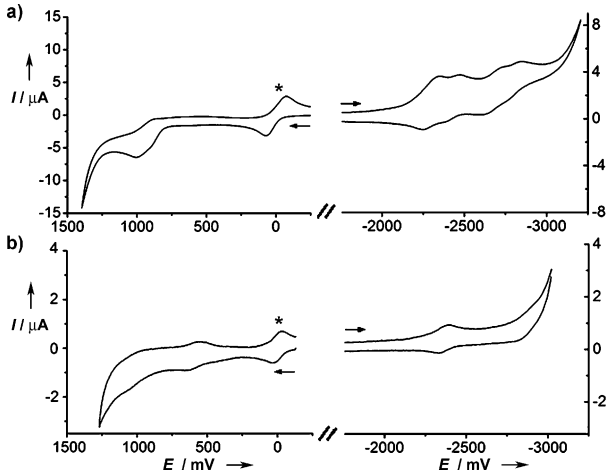

Figure 4. Cyclic voltammetry plots for a) **MC1** and b) **MC2**. Reductions (right) in THF and oxidations (left) in CH_2Cl_2 containing 0.1 M Bu_4NPF_6; recorded vs Fc^+/Fc at a scan rate of 100 mVs^{-1}. Fc as an internal reference is indicated with an asterisk.

MC1, which suggests that the individual boron atoms communicate with each other through the π-bridges in the cycle. In contrast, the boron atoms in **MC2** are reduced simultaneously, indicating no mutual interaction due to the greater spatial separation and lack of orbital overlap. The first reductions at −2.30 V for **MC1** and −2.33 V for **MC2** reveal that these macrocycles are more easily reduced compared with **MC-B3N3** (−2.53 V). The HOMO–LUMO energy gaps of 3.25 eV and 2.94 eV for **MC1** and **MC2** estimated from electrochemical data are reasonably consistent with data from UV/Vis measurements and DFT calculations (Table 1).

Table 1: Comparison of experimental data and computed frontier orbital energies for **MC1** and **MC2**.

		CV[a] [eV]	SWV[a] [eV]	DFT[b] [eV]	UV/Vis[c] [nm] (*E* [eV])	TDDFT[b] [nm] (*E* [eV])
MC1	E_{LUMO}	−2.50	−2.50	−1.87		
	E_{HOMO}	−5.75	−5.75	−5.41		
	ΔE_{gap}	3.25	3.25	3.54	390 (3.18)	382 (3.24)[d]
MC2	E_{LUMO}	−2.43	−2.47	−1.77		
	E_{HOMO}	−5.40	−5.41	−5.06		
	ΔE_{gap}	2.97	2.94	3.29	427 (2.90)	409 (3.03)[d]

[a] Reference: ferrocene at 4.80 eV below vacuum; CV = cyclic voltammetry, SWV = square-wave voltammetry (Supporting Information, Figure S18). [b] Computations performed on simplified analogues of **MC1** and **MC2**. [c] Onset of the UV/Vis absorption spectra. [d] Allowed $S_2 \leftarrow S_0$ transition.

Finally, the ability of **MC1** to act as a Lewis acid host for anions was explored by monitoring the changes in the UV/Vis absorption and emission spectra upon cyanide addition. Gradual addition of two equivalents of CN^- to a solution of **MC1** in toluene led to a decrease in intensity of the major absorption band at 361 nm and subsequent splitting into two absorptions of similar intensity at 356 and 378 nm (Figure 5a). At the same time, the emission bands at 430 and 408 nm decreased, giving way to a single broad feature at 430 nm. The emission maximum for $[\mathbf{MC1}(CN)_2]^{2-}$ appeared much more bathochromic at ca. 475 nm in CH_2Cl_2 as a more polar solvent (Supporting Information, Figure S19), suggesting a solvatochromic effect due to further enhanced charge transfer character upon anion complexation. In the presence of much larger amounts of CN^- the absorption and emission bands disappeared, giving way to higher energy absorptions at 308 and 327 nm and a structured emission at ca. 369 nm. These spectral features are attributed to π–π* transitions of the fully complexed species $[\mathbf{MC1}(CN)_4]^{4-}$ with contributions from both the carbazole and fluorene moieties.

Fitting of the absorption data to four separate binding events ($\lg\beta_{11} = 7.5$, $\lg\beta_{12} = 14.5$, $\lg\beta_{13} = 20.8$, $\lg\beta_{14} = 27.0$) revealed very large stepwise binding constants (Supporting Information, Figure S20). Cooperative effects were not observed in toluene as the individual binding constants are similar, possibly reflecting the limit of the measurable binding strength. Indeed, in the more polar solvent CH_2Cl_2, complexation of the first two cyanide anions was also very strong, but

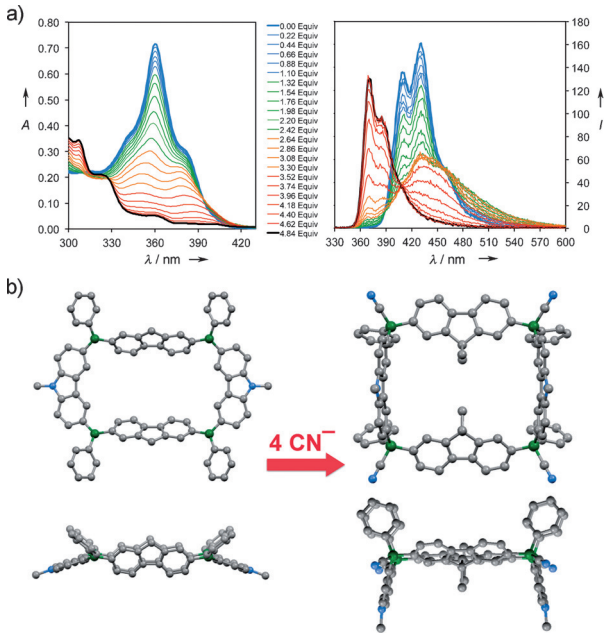

Figure 5. a) Titration of **MC1** with CN^- (9.7×10^{-4} M) in toluene, monitored by UV/Vis and fluorescence spectroscopy. [**MC1**] = 8.4×10^{-6} M; λ_{exc} = 320 nm. b) Illustration of the predicted shape changes for **MC1** upon anion binding.

relatively smaller binding constants were detected for the last two cyanides.

Geometry optimization of the possible isomers of $[\mathbf{MC1}(CN)_2]^{2-}$ revealed that boron complexation at opposite corners of the macrocycle is energetically most favorable (Supporting Information, Figure S13). The narrowing of the endocyclic C-B-C angles triggers a reversal of the orientation of the fluorene moieties relative to the free acid, such that the methylenes (C9 positions) point towards the center. The same is true for the energetically most favorable isomer of $[\mathbf{MC1}(CN)_4]^{4-}$, in which all four cyanides are oriented in the same direction. An especially interesting aspect is that, upon anion binding, the structure of the macrocycle changes from an elongated to a more square-like shape (Figure 5b), which is reflected in a decrease of the trans-annular N···N separations from 17.6 to 13.7 (2 CN^-) and 12.3 Å (4 CN^-).

In conclusion, we introduce a versatile design principle for B/N containing ambipolar macrocycles with new shapes and sizes. The ambipolar nature of the macrocycles **MC1** and **MC2** is reflected in solvatochromic emission effects that are most pronounced in **MC2**. Electronic communication between the fluorene-bridged borane moieties in **MC1** results in splitting of the electrochemical redox waves and a reduced LUMO orbital level relative to the C_3-symmetric analogue **MC-B3N3**. Complexation of cyanide anions to **MC1** triggers a unique anion response, including changes in the macrocycle geometry and the appearance of strong charge transfer bands for the bis(cyanide) complex. We envision that the new modular synthetic routes to boron-containing macrocycles will encourage further exploration of this unusual class of materials as not only different shapes and sizes become accessible, but also other functional building blocks are readily incorporated.

Keywords: ambipolar macrocycles · anion binding · luminescence · organoboranes · π-conjugation

How to cite: *Angew. Chem. Int. Ed.* **2015**, *54*, 10768 – 10772
Angew. Chem. **2015**, *127*, 10918 – 10922

[1] a) Special issue on Organic Electronics and Optoelectronics in *Chem. Rev.* **2007**, *107*, 923 – 1386; b) Special issue on Organic Photovoltaics in *Acc. Chem. Res.* **2009**, *42*, 1689 – 1857; c) S. W. Thomas III, G. D. Joly, T. M. Swager, *Chem. Rev.* **2007**, *107*, 1339 – 1386.

[2] a) L. Zang, Y. Che, J. S. Moore, *Acc. Chem. Res.* **2008**, *41*, 1596 – 1608; b) R. R. Tykwinski, M. Gholami, S. Eisler, Y. Zhao, F. Melin, L. Echegoyen, *Pure Appl. Chem.* **2008**, *80*, 621 – 637; c) M. Iyoda, J. Yamakawa, M. J. Rahman, *Angew. Chem. Int. Ed.* **2011**, *50*, 10522 – 10553; *Angew. Chem.* **2011**, *123*, 10708 – 10740.

[3] a) Y. Xu, M. D. Smith, J. A. Krause, L. S. Shimizu, *J. Org. Chem.* **2009**, *74*, 4874 – 4877; b) S. Höger, *Pure Appl. Chem.* **2010**, *82*, 821 – 830; c) D. Ramaiah, P. P. Neelakandan, A. K. Nair, R. R. Avirah, *Chem. Soc. Rev.* **2010**, *39*, 4158 – 4168; d) T. Iwamoto, Y. Watanabe, T. Sadahiro, T. Haino, S. Yamago, *Angew. Chem. Int. Ed.* **2011**, *50*, 8342 – 8344; *Angew. Chem.* **2011**, *123*, 8492 – 8494; e) F. E. Golling, M. Quernheim, M. Wagner, T. Nishiuchi, K. Müllen, *Angew. Chem. Int. Ed.* **2014**, *53*, 1525 – 1528; *Angew. Chem.* **2014**, *126*, 1551 – 1554.

[4] a) G. R. Newkome, H. W. Lee, *J. Am. Chem. Soc.* **1983**, *105*, 5956 – 5957; b) F. H. Carré, R. J.-P. Corriu, T. Deforth, W. E. Douglas, W. S. Siebert, W. Weinmann, *Angew. Chem. Int. Ed.* **1998**, *37*, 652 – 653; *Angew. Chem.* **1998**, *110*, 654 – 656; c) P. Jutzi, N. Lenze, B. Neumann, H.-G. Stammler, *Angew. Chem. Int. Ed.* **2001**, *40*, 1423 – 1427; *Angew. Chem.* **2001**, *113*, 1469 – 1473; d) C. Burress, C. Elbjeirami, M. A. Omary, F. P. Gabbai, *J. Am. Chem. Soc.* **2005**, *127*, 12166 – 12167; e) V. H. Gessner, J. F. Tannaci, A. D. Miller, T. D. Tilley, *Acc. Chem. Res.* **2011**, *44*, 435 – 446; f) P. F. Wei, T. R. Cook, X. H. Yan, F. H. Huang, P. J. Stang, *J. Am. Chem. Soc.* **2014**, *136*, 15497 – 15500; g) J. M. Ludlow III, M. Tominaga, Y. Chujo, A. Schultz, X. C. Lu, T. Z. Xie, K. Guo, C. N. Moorefield, C. Wesdemiotis, G. R. Newkome, *Dalton Trans.* **2014**, *43*, 9604 – 9611; h) T. Z. Xie, S. Y. Liao, K. Guo, X. C. Lu, X. H. Dong, M. J. Huang, C. N. Moorefield, S. Z. D. Cheng, X. Liu, C. Wesdemiotis, G. R. Newkome, *J. Am. Chem. Soc.* **2014**, *136*, 8165 – 8168.

[5] a) A. Ito, Y. Yokoyama, R. Aihara, K. Fukui, S. Eguchi, K. Shizu, T. Sato, K. Tanaka, *Angew. Chem. Int. Ed.* **2010**, *49*, 8205 – 8208; *Angew. Chem.* **2010**, *122*, 8381 – 8384; b) D. Sakamaki, A. Ito, K. Furukawa, T. Kato, M. Shiro, K. Tanaka, *Angew. Chem. Int. Ed.* **2012**, *51*, 12776 – 12781; *Angew. Chem.* **2012**, *124*, 12948 – 12953.

[6] See also: a) M.-X. Wang, X.-H. Zhang, Q.-Y. Zheng, *Angew. Chem. Int. Ed.* **2004**, *43*, 838 – 842; *Angew. Chem.* **2004**, *116*, 856 – 860; b) E.-X. Zhang, D.-X. Wang, Q.-Y. Zheng, M.-X. Wang, *Org. Lett.* **2008**, *10*, 2565 – 2568; c) T. F. Yang, K. Y. Chiu, H. C. Cheng, Y. W. Lee, M. Y. Kuo, Y. O. Su, *J. Org. Chem.* **2012**, *77*, 8627 – 8633; d) Y. Yokoyama, D. Sakamaki, A. Ito, K. Tanaka, M. Shiro, *Angew. Chem. Int. Ed.* **2012**, *51*, 9403 – 9406; *Angew. Chem.* **2012**, *124*, 9537 – 9540; e) D. Sakamaki, A. Ito, K. Furukawa, T. Kato, K. Tanaka, *J. Org. Chem.* **2013**, *78*, 2947 – 2956.

[7] F. P. Gabbaï, *Angew. Chem. Int. Ed.* **2003**, *42*, 2218 – 2221; *Angew. Chem.* **2003**, *115*, 2318 – 2321.

[8] P. Chen, F. Jäkle, *J. Am. Chem. Soc.* **2011**, *133*, 20142 – 20145.

[9] P. Chen, R. A. Lalancette, F. Jäkle, *Angew. Chem. Int. Ed.* **2012**, *51*, 7994 – 7998; *Angew. Chem.* **2012**, *124*, 8118 – 8122.

[10] a) C. D. Entwistle, T. B. Marder, *Angew. Chem. Int. Ed.* **2002**, *41*, 2927 – 2931; *Angew. Chem.* **2002**, *114*, 3051 – 3056; b) C. D. Entwistle, T. B. Marder, *Chem. Mater.* **2004**, *16*, 4574 – 4585; c) G. Zhou, M. Baumgarten, K. Müllen, *J. Am. Chem. Soc.* **2008**, *130*, 12477 – 12484; d) C. R. Wade, A. E. J. Broomsgrove, S. Aldridge, F. P. Gabbai, *Chem. Rev.* **2010**, *110*, 3958 – 3984; e) F. Jäkle, *Chem. Rev.* **2010**, *110*, 3985 – 4022; f) K. Tanaka, Y. Chujo, *Macromol. Rapid Commun.* **2012**, *33*, 1235 – 1255; g) C. V. Hoven, H. P. Wang, M. Elbing, L. Garner, D. Winkelhaus, G. C. Bazan, *Nat. Mater.* **2010**, *9*, 249 – 252; h) H. C. Schmidt, L. G. Reuter, J. Hamacek, O. S. Wenger, *J. Org. Chem.* **2011**, *76*, 9081 – 9085; i) S. Saito, K. Matsuo, S. Yamaguchi, *J. Am. Chem. Soc.* **2012**, *134*, 9130 – 9133; j) M. Steeger, C. Lambert, *Chem. Eur. J.* **2012**, *18*, 11937 – 11948; k) A. J. V. Marwitz, A. N. Lamm, L. N. Zakharov, M. Vasiliu, D. A. Dixon, S. Y. Liu, *Chem. Sci.* **2012**, *3*, 825 – 829; l) B. Neue, J. F. Araneda, W. E. Piers, M. Parvez, *Angew. Chem. Int. Ed.* **2013**, *52*, 9966 – 9969; *Angew. Chem.* **2013**, *125*, 10150 – 10153; m) C. Reus, S. Weidlich, M. Bolte, H.-W. Lerner, M. Wagner, *J. Am. Chem. Soc.* **2013**, *135*, 12892 – 12907; n) H. Braunschweig, V. Dyakonov, B. Engels, Z. Falk, C. Hörl, J. H. Klein, T. Kramer, H. Kraus, I. Krummenacher, C. Lambert, C. Walter, *Angew. Chem. Int. Ed.* **2013**, *52*, 12852 – 12855; *Angew. Chem.* **2013**, *125*, 13088 – 13092; o) C. T. Poon, W. H. Lam, V. W. W. Yam, *Chem. Eur. J.* **2013**, *19*, 3467 – 3476; p) Y. L. Rao, C. Hörl, H. Braunschweig, S. N. Wang, *Angew. Chem. Int. Ed.* **2014**, *53*, 9086 – 9089; *Angew. Chem.* **2014**, *126*, 9232 – 9236; q) D. R. Levine, M. A. Siegler, J. D. Tovar, *J. Am. Chem. Soc.* **2014**, *136*, 7132 – 7139; r) X. D. Yin, J. W. Chen, R. A. Lalancette, T. B. Marder, F. Jäkle, *Angew. Chem. Int. Ed.* **2014**, *53*, 9761 – 9765; *Angew. Chem.* **2014**, *126*, 9919 – 9923; s) Z. L. Zhang, R. M. Edkins, J. Nitsch, K. Fucke, A. Steffen, L. E. Longobardi, D. W. Stephan, C. Lambert, T. B. Marder, *Chem. Sci.* **2015**, *6*, 308 – 321; t) X. Wang, Y. L. Chang, J. S. Lu, T. Zhang, Z. H. Lu, S. N. Wang, *Adv. Funct. Mater.* **2014**, *24*, 1911 – 1927; u) P. C. A. Swamy, P. Thilagar, *Inorg. Chem.* **2014**, *53*, 2776 – 2786; v) X. Y. Wang, F. D. Zhuang, R. B. Wang, X. C. Wang, X. Y. Cao, J. Y. Wang, J. Pei, *J. Am. Chem. Soc.* **2014**, *136*, 3764 – 3767; w) T. Hatakeyama, S. Hashimoto, S. Seki, M. Nakamura, *J. Am. Chem. Soc.* **2011**, *133*, 18614 – 18617; x) X. Y. Li, X. D. Guo, L. X. Cao, Z. Q. Xun, S. Q. Wang, S. Y. Li, Y. Li, G. Q. Yang, *Angew. Chem. Int. Ed.* **2014**, *53*, 7809 – 7813; *Angew. Chem.* **2014**, *126*, 7943 – 7947.

[11] a) S. Yamago, Y. Watanabe, T. Iwamoto, *Angew. Chem. Int. Ed.* **2010**, *49*, 757 – 759; *Angew. Chem.* **2010**, *122*, 769 – 771; b) E. Kayahara, V. K. Patel, S. Yamago, *J. Am. Chem. Soc.* **2014**, *136*, 2284 – 2287; c) T. Iwamoto, E. Kayahara, N. Yasuda, T. Suzuki, S. Yamago, *Angew. Chem. Int. Ed.* **2014**, *53*, 6430 – 6434; *Angew. Chem.* **2014**, *126*, 6548 – 6552.

[12] F. P. Gabbaï, *Angew. Chem. Int. Ed.* **2012**, *51*, 6316 – 6318; *Angew. Chem.* **2012**, *124*, 6423 – 6425.

[13] M. J. Frisch et al., Gaussian 09, Revision B.01, Inc., Wallingford, CT, **2010**.

[14] a) M. Bednarz, P. Reineker, E. Mena-Osteritz, P. Bäuerle, *J. Lumin.* **2004**, *110*, 225 – 231; b) M. Hoffmann, J. Kärnbratt, M.-H. Chang, L. M. Herz, B. Albinsson, H. L. Anderson, *Angew. Chem. Int. Ed.* **2008**, *47*, 4993 – 4996; *Angew. Chem.* **2008**, *120*, 5071 – 5074; c) J. K. Sprafke, D. V. Kondratuk, M. Wykes, A. L. Thompson, M. Hoffmann, R. Drevinskas, W. H. Chen, C. K. Yong, J. Karnbratt, J. E. Bullock, M. Malfois, M. R. Wasielewski, B. Albinsson, L. M. Herz, D. Zigmantas, D. Beljonne, H. L. Anderson, *J. Am. Chem. Soc.* **2011**, *133*, 17262 – 17273.

Received: April 8, 2015
Published online: June 26, 2015